Guest-Responsive Near-Infrared Luminescent Metal–Organic Cage Organized by Porphyrin Dye and Yb(III) Complex

Shota Hosoya,[1] Sunao Shoji,[2,3,4,*] Takayuki Nakanishi,[5] Masato Kobayashi,[2,6], Mengfei Wang,[2,3] Koji Fushimi,[3] Tetsuya Taketsugu,[2,6] Yuichi Kitagawa,[2,3] Yasuchika Hasegawa[2,3,*]

[1]Graduate School of Chemical Sciences and Engineering, Hokkaido University, Kita 13, Nishi 8, Kita-ku, Sapporo, Hokkaido 060-8628, Japan.

[2]Institute for Chemical Reaction Design and Discovery (WPI-ICReDD), Hokkaido University, Kita 21, Nishi 10, Kita-ku, Sapporo, Hokkaido 001-0021, Japan.

[3]Faculty of Engineering, Hokkaido University, Kita 13, Nishi 8, Kita-ku, Sapporo, Hokkaido 060-8628, Japan.

[4]Present address: Faculty of Engineering, Nara Women's University, Kitauoya-Nishimachi, Nara 630-8506, Japan.

[5]Research Center for Electronic and Optical Materials, National Institute for Materials Science (NIMS), 1-1 Namiki, Tsukuba, Ibaraki 305-0044, Japan.

[6]Department of Chemistry, Faculty of Science, Hokkaido University, Kita 10, Nishi 8, Kita-ku, Sapporo, Hokkaido 060-0810, Japan.

Received: April 2024
Revised: May 2024
Published:

ABSTRACT: Metal–organic cages (MOCs) with luminophores have significant advantages for the facile detection of specific molecules based on turn-on or turn-off luminescence changes induced by host–guest complexation. One important challenge is the development of turn-on-type near-infrared (NIR)-luminescent MOCs. In this study, we synthesized a novel MOC consisting of two porphyrin dyes linked by four Yb(III) complexes, which exhibits bimodal red and NIR fluorescence signals upon photoexcitation of the porphyrin π-system. Single-crystal X-ray structural analysis and computational molecular modelling revealed that planar aromatic perfluorocarbons were intercalated into the MOC. The tight packing between the MOC and guests enhanced the NIR fluorescence of the Yb(III) by suppressing energy transfer from the photoexcited porphyrin to oxygen molecules. Guest-responsive turn-on NIR fluorescence changes in a MOC were successfully demonstrated.

Metal–organic cages (MOCs) organized by coordination-driven self-assembly have attracted great attention in the field of supramolecular chemistry[1–3] because of their potential applications for sensors,[4,5] catalysts,[6,7] molecular separations,[8,9] and biological technologies.[10,11] In particular, MOCs with luminophores have significant advantages for the development of systems for the facile detection of specific molecules based on turn-on or turn-off luminescence changes of the host and/or guest molecules through supramolecular complexation.[5,12,13] Although many luminescent MOCs have been reported, there have been limited studies on near-infrared (NIR)-emitting MOCs.[14–16] NIR-luminescent MOCs are highly desirable for biosensing applications because NIR light can penetrate deeply into biological tissues.[17] However, the development of turn-on-type NIR-luminescent MOCs with molecular recognition ability remains a challenge.

Trivalent lanthanide ions (Ln(III)) are an important class for building photo-functional MOCs.[18] Among the Ln(III) ions, the Yb(III) exhibits long-lived NIR emission based on 4f–4f transitions, and its complexes have been widely studied for luminescent probes.[19] They can effectively produce NIR fluorescence through energy transfer from the excited triplet state (T_1) of the organic ligands to the Yb(III) ion.[20] Porphyrin derivatives, which have strong visible light absorption and an appropriate T_1 level, are excellent candidates as photosensitizers for the Yb(III).[15,21–25] Furthermore, porphyrin-based ligands are well-known building blocks with versatile utility to construct cage-like assemblies owing to the stiffness and symmetry of their aromatic core.[26–28] A Yb(III) complex with the porphyrin-assembled MOC system has been demonstrated for NIR-fluorescence sensor.[15]

In this study, we synthesized a novel NIR-emissive MOC composed of $Yb(hfa)_3$ (hfa: hexafluoroacetylacetonato) complexes and a free-base porphyrin containing four triphenylphosphine oxide units (Figure 1a). The combination of $Ln(hfa)_3$ and phosphine oxides is useful for the molecular design of luminescent Ln(III) coordination compounds.[29–31] The phosphine oxide group also functions as a spacer between porphyrin

and Yb(III) and suppresses the heavy-atom effect of the Yb(III) ion,[32,33] resulting in bimodal emission of the porphyrin and Yb(III). The developed MOC was able to encapsulate planar aromatic perfluorocarbons such as hexafluorobenzene (HFB) or octafluoronaphthalene (OFN) (Figure 1b). In the presence of these guest molecules, the MOC showed a ratiometric fluorescence change with an increase in the NIR fluorescence of the Yb(III). Herein, we demonstrated the guest-responsive turn-on NIR fluorescence changes in the MOC with porphyrin dyes and Yb(III) ions.

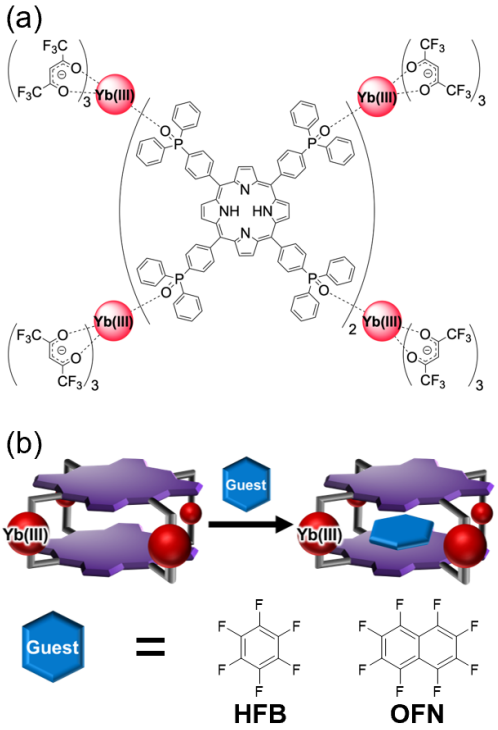

Figure 1. (a) Molecular structure of $[Yb_4(hfa)_{12}(PorTPPO)_2]$. (b) Schematic illustration of host–guest complexation.

A porphyrin ligand with four 4-(diphenylphosphoryl)phenyl groups at the *meso*-positions, PorTPPO, was synthesized according to the reported method.[34] PorTPPO was mixed with the precursor complex $[Yb(hfa)_3(H_2O)_2]$[29,30] in a mixed solvent of $CHCl_3$ and alcohol (MeOH or *i*-PrOH) to give a crystalline coordination compound, $[Yb_4(hfa)_{12}(PorTPPO)_2]$ (Figure S1). Single-crystal X-ray diffraction (SCXRD) analysis

revealed a cage-like framework consisting of two cofacial free-base porphyrins linked by four $Yb(hfa)_3$ complexes (Figure 3a/b). The distance between the porphyrin π-planes was found to be 7.56 Å, and the size of the cavity was estimated to be approximately 300 $Å^3$ (Figure S2). The coordination of Yb(III) comprises eight oxygen atoms of three hfa and two phosphine oxides of PorTPPO. Continuous shape measures (CShM) analysis was performed to clarify the coordination geometry of Yb(III). The coordination structure was characterized as two types of eight-coordinated square antiprismatic (SARP-8) structures in a cage molecule (Figure S7 and Table S2). The powder XRD pattern coincided with the simulated peaks using the SCXRD data, suggesting that the obtained powder was uniform without polymorphic structures (Figure S3). Elemental analysis and FT-IR also indicated that $[Yb_4(hfa)_{12}(PorTPPO)_2]$ was successfully synthesized (Figure S4).

The UV-Vis absorption spectrum of $[Yb_4(hfa)_{12}(PorTPPO)_2]$ in $CHCl_3$ solution showed Soret band at 416 nm and Q bands at 514, 550, 589, and 645 nm, as well as the π–π* transition of hfa at 307 nm (Figure 2a). The absorption peaks of the porphyrin moiety were slightly blue-shifted compared to those of PorTPPO (Soret band at 422 nm and Q bands at 517, 552, 590, and 647 nm). The concentration-dependent UV-Vis absorption of $[Yb_4(hfa)_{12}(PorTPPO)_2]$ was measured in the range of 2.0 to 0.4 μM (Figure S10). The absorption maxima of the Soret and Q bands shifted bathochromically at lower concentrations due to dissociation of the MOC framework by dilution, whereas the MOC structure is preserved at concentrations above 1.2 μM. ESI-MS analysis provided further evidence of the presence of the MOC in solution (Figure 2b).

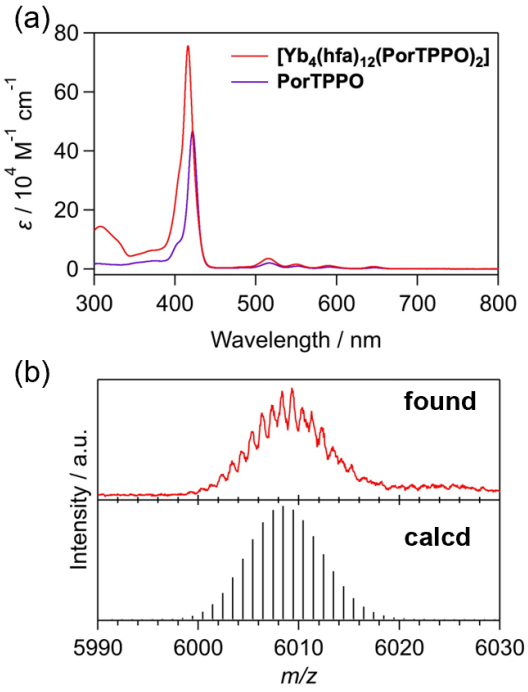

Figure 2. (a) UV-Vis absorption spectra of PorTPPO (5 μM, purple line) and $[Yb_4(hfa)_{12}(PorTPPO)_2]$ (2.5 μM, red line) in $CHCl_3$. (b) ESI-MS of $\{[Yb_4(hfa)_{12}(PorTPPO)_2]+H\}^+$.

Cage-like compounds containing two parallelly arranged aromatics at a well-defined distance are known as versatile host materials that can intercalate aromatic guests through non-covalent π–π interactions.[26,27,35–38] In particular, cofacial porphyrin cage shows strong intercalation with electron-deficient guests.[38] The computational molecular modelling based on a semi-empirical GFN-xTB method[39] is useful for determining the optimized structure and stabilization energy of large host–guest supramolecules with a certain accuracy,[40] in comparison to the density functional theory that takes enormous computational time for geometry optimization. We performed the geometry optimizations of the host–guest complexes of $[Yb_4(hfa)_{12}(PorTPPO)_2]$ and small aromatic derivatives with different numbers of electron-withdrawing fluorine substituents by the GFN2-xTB level of calculations and investigated the interaction energies. The stabilization energy of the 1:1 host–guest complexation (ΔE_{stab}) was obtained as the energy difference between

the host–guest complex ($E_{\text{host-guest}}$) and its isolated components (E_{host} and E_{guest}). Based on the systematic calculations, a clear trend with increasing number of fluorine substituents could be observed for both benzene and naphthalene derivatives (Figure S18 and Tables S5–6). When molecules possess a greater number of fluorine substituents and a larger π-surface, the guests become more electron-deficient, resulting in a greater ΔE_{stab} compared to aromatic hydrocarbons. The computational modelling suggested that aromatic perfluorocarbons are suitable guests for $[Yb_4(hfa)_{12}(PorTPPO)_2]$.

In contrast to the low solubility of $[Yb_4(hfa)_{12}(PorTPPO)_2]$ in various organic solvents, a significantly higher solubility was observed in a $CHCl_3$ solution containing HFB or OFN (Figure S5). Single crystals were obtained via recrystallization from $CHCl_3$ solutions of $[Yb_4(hfa)_{12}(PorTPPO)_2]$ mixed with HFB or OFN. The SCXRD analysis indicated that HFB and OFN were encapsulated in the cage to form the 1:1 host–guest complexes, $[Yb_4(hfa)_{12}(PorTPPO)_2]\supset$HFB and $[Yb_4(hfa)_{12}(PorTPPO)_2]\supset$OFN (Figure 3c–f). The alignments of the cofacial porphyrins and the coordination geometries of $Yb(hfa)_3$ were altered slightly by the host–guest complexation (Figures S6–S9 and Tables S2–S4). The distances between the porphyrin π-planes of the cages with HFB and OFN were found to be 6.92 and 6.71 Å, respectively (Figures 3d/f and S6). The shortened distances can be attributed to the stronger π–π interactions of the porphyrins and encapsulated guests. The π–π interactions of the host–guest complexes were also confirmed using a non-covalent interaction (NCI) plot (Figures S19–S20).[41] These results indicated that planar aromatic perfluorocarbons have strong electrostatic interactions with the double-decker structure of the electron-rich porphyrins to give tight packing, which is in agreement with the computational modelling.

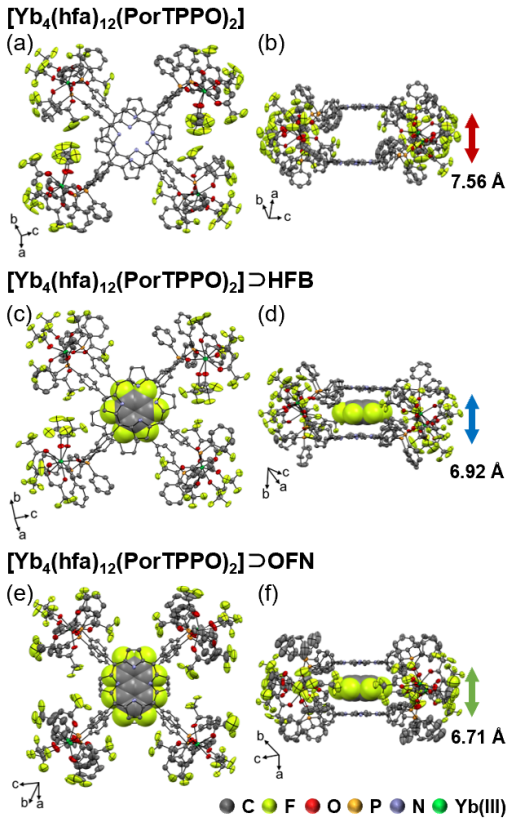

Figure 3. Crystal structures of (a/b) $[Yb_4(hfa)_{12}(PorTPPO)_2]$, (c/d) $[Yb_4(hfa)_{12}(PorTPPO)_2]\supset$HFB, and (e/f) $[Yb_4(hfa)_{12}(PorTPPO)_2]\supset$OFN (a/c/e: top view, b/d/f: side view). Ellipsoids were drawn at 50% probability and hydrogen atoms were omitted for clarity.

The host–guest complexation of $[Yb_4(hfa)_{12}(PorTPPO)_2]$ in $CHCl_3$ was also confirmed using UV-Vis absorption and ESI-MS. The UV-Vis absorption spectra of $[Yb_4(hfa)_{12}(PorTPPO)_2]$ showed a slight absorption change in the presence of HFB or OFN (Figure S11). In contrast, $[Yb_4(hfa)_{12}(PorTPPO)_2]$ exhibited almost identical spectra in a solution with benzene, naphthalene, hexane, or perfluorohexane (Figure S12). The absorption changes might be attribute to a slight influence on the electronic structure of the ground state of porphyrin induced by alternation of the surrounding environment from chloroform to guest molecules. The ESI-MS showed peaks corresponding to $\{[Yb_4(hfa)_{12}(PorTPPO)_2]\supset OFN+H\}^+$ (Figure 4a), indicating that the 1:1 host–guest complex was formed in $CHCl_3$. Unfortunately, the mass peaks of the

$[Yb_4(hfa)_{12}(PorTPPO)_2]\supset$HFB species were not observed, probably due to its weak binding.

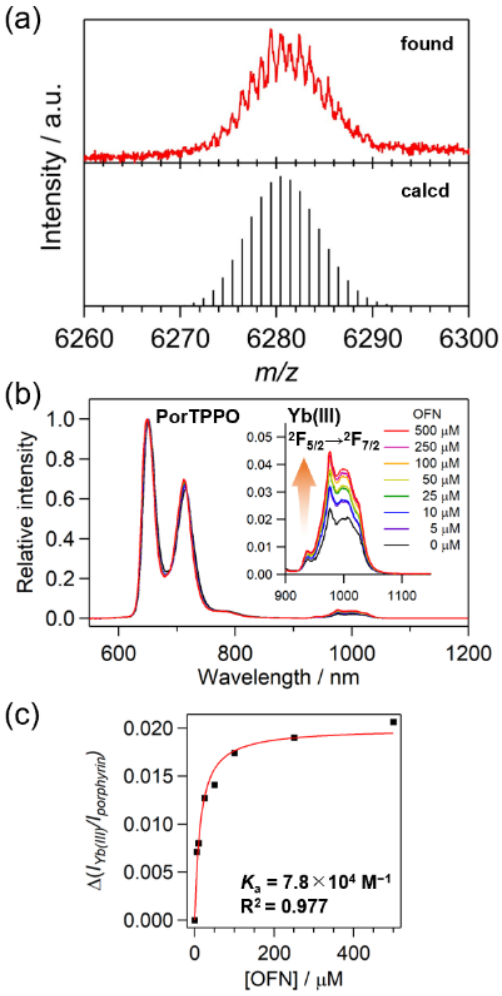

Figure 4. (a) ESI-MS of $\{[Yb_4(hfa)_{12}(PorTPPO)_2]\supset OFN+H\}^+$. (b) Emission spectra ($\lambda_{ex}$ = 415 nm) of 2.5 μM $[Yb_4(hfa)_{12}(PorTPPO)_2]$ in $CHCl_3$ with different concentrations of OFN at r.t., and (c) plots of the relative fluorescence changes ($\Delta(I_{Yb(III)}/I_{porphyrin})$) and fitting curve according to the 1:1 host–guest model.

The emission properties of the MOC were investigated for the present supramolecular host–guest system in $CHCl_3$ solution under air and Ar atmospheres. Upon selective photoexcitation of the porphyrin at the Soret band in air, $[Yb_4(hfa)_{12}(PorTPPO)_2]$ exhibited bimodal fluorescence originating from the porphyrin

and Yb(III) (Figure 4b, black line). The fluorescence peaks of the porphyrin moiety were observed at 651 and 715 nm, and that of the Yb(III) ion ($^2F_{5/2}\rightarrow{}^2F_{7/2}$) was found at around 1000 nm. The excitation spectrum for the NIR emission was similar to the UV-Vis absorption spectrum, indicating that the porphyrin dye photosensitized the Yb(III) ions (Figure S13). The fluorescence quantum yields of porphyrin ($\Phi_{\text{porphyrin}}$) and Yb(III) ($\Phi_{\text{Yb(III)}}$) were determined to be 5.5% and 0.3%, respectively (Table 1).

Table 1. Photophysical properties of $[Yb_4(hfa)_{12}(PorTPPO)_2]$.

Guest	$\tau_{\text{Yb(III)}}$ / μs	[a]$\Phi_{\text{4f-4f}}$ / %	under air			under Ar		
			$\Phi_{\text{porphyrin}}$ / %	$\Phi_{\text{Yb(III)}}$ / %	η_{sens} / %	$\Phi_{\text{porphyrin}}$ / %	$\Phi_{\text{Yb(III)}}$ / %	η_{sens} / %
no guest	22	3.0	5.5	0.3	10	6.4	1.9	63
HFB	22	3.0	5.8	0.5	17	6.8	1.9	63
OFN	22	3.0	6.0	0.7	23	6.7	1.8	60

[a]Estimated from $[Yb(hfa)_3(TPPO)_2]$ (TPPO: triphenylphosphine oxide)[29] using Strickler–Berg equation (see Supporting Information 5-3).

The guest-concentration-dependent emission spectra showed that the fluorescence intensity of the Yb(III) gradually increased upon the addition of OFN or HFB, whereas that of the porphyrin remained almost constant (Figures 4b and S14a). In the presence of 100 μM OFN or 100 mM HFB, $\Phi_{\text{Yb(III)}}$ increased to 0.7% and 0.5%, respectively. The association constants (K_a) of the cage were estimated from the change in the fluorescence intensity of the Yb(III) to relative to that of porphyrin ($\Delta(I_{\text{Yb(III)}}/I_{\text{porphyrin}})$) at room temperature. Based on the spectral changes, K_a values were calculated using non-linear curve fitting according to the 1:1 host–guest binding model.[42] The K_a values of the MOC with OFN and HFB were found to be 7.8×10^4 and 1.6×10^2 M^{-1}, respectively, indicating that OFN was intercalated stronger (Figures 4c and S14b).

After bubbling Ar gas into the solution to remove dissolved oxygen molecules, the $\Phi_{\text{Yb(III)}}$ value of the MOC, with or without guests, increased significantly to 1.9%

(Figure S15). This evidence indicates that the energy transfer from porphyrin to Yb(III) is promoted by suppression of oxygen quenching. The slight increase of $\Phi_{porphyrin}$ can be also attribute to removal of oxygen molecules.[43] The NIR-emission lifetimes of the Yb(III) showed a single-exponential decay of 22 μs (Figure S16). The intrinsic quantum yield of the Yb(III) ($\Phi_{4f\text{-}4f}$) was calculated to be 3.0% using the Strickler–Berg equation (see Supporting Information 5-3). These values remained consistent, regardless of the presence or absence of guests. The energy transfer efficiency from porphyrin to the Yb(III) ion ($\eta_{sens} = \Phi_{Yb(III)}/\Phi_{4f\text{-}4f}$) was determined to be 10% in a $CHCl_3$ solution under air. With the presence of guests in this solution, η_{sens} increased to 23% and 17% for OFN (100 μM) and HFB (100 mM), respectively. After bubbling Ar gas through the solutions, the η_{sens} values of all the samples increased to 60–63%. The consistent photophysical data of the Yb(III) in the presence or absence of guests under the Ar-saturated conditions revealed that the guest molecules rarely affect to the 4f-4f emission characteristics of the Yb(III).

We considered that the guest-responsive turn-on NIR fluorescence enhancement in air conditions was attributed to oxygen blocking by the formation of a tight host-guest complex. The structural protection of the ligand π-surface in the luminescent Ln(III) complexes is a key strategy for suppression of the oxygen quenching.[44] The higher energy transfer efficiency of the MOC with guests in air can be explained by the stronger intercalation and larger cover of the porphyrin π-surface.

In summary, we successfully synthesized a novel NIR-luminescent, bimodal, and guest-responsive turn-on MOC composed of porphyrin dyes and Yb(III) complexes. The MOC has a well-defined three-dimensional cavity, and small planar aromatic perfluorocarbons were intercalated inside the cage to form 1:1 host–guest supramolecules. The tight host-guest packing partially inhibited oxygen molecules from approaching the cage and increased the NIR fluorescence of Yb(III). The supramolecular engineering based on the tightly packed cage structure and oxygen blocking strategy represents a new

approach towards photofunctional host materials for future biological probes. We expect that this study will stimulate the design and synthesis of new NIR-emissive MOCs for practical applications.

■ ASSOCIATED CONTENT

Supporting Information

The Supporting Information is available free of charge at https://pubs.acs.org/doi/10.1021/acs.inorgchem.

Experimental details, spectroscopic data, X-ray crystallography, computational molecular modelling, and additional information (PDF)

Accession Codes

CCDC 2326295 (for $[Yb_4(hfa)_{12}(PorTPPO)_2]$), 2326296 (for $[Yb_4(hfa)_{12}(PorTPPO)_2]\supset$HFB), and 2326297 (for $[Yb_4(hfa)_{12}(PorTPPO)_2]\supset$OFN) contain the supplementary crystallographic data for this paper. These data can be obtained free of charge via www.ccdc.cam.ac.uk/data_request/cif, by emailing data_request@ccdc.cam.ac.uk, or by contacting The Cambridge Crystallographic Data Centre, 12 Union Road, Cambridge CB2 1EZ, UK; fax: +441223 336033.

■ AUTHOR INFORMATION

Corresponding Authors

Sunao Shoji – *Faculty of Engineering, Hokkaido University, Sapporo, Hokkaido 060-8628, Japan; Institute for Chemical Reaction Design and Discovery (WPI-ICReDD), Hokkaido University, Sapporo, Hokkaido 001-0021, Japan;* Present Address: Faculty of Engineering, Nara Women's University, Nara 630-8506, Japan; orcid.org/0000-0002-0329-1136; Email: shoji@cc.nara-wu.ac.jp

Yasuchika Hasegawa – *Faculty of Engineering, Hokkaido University, Sapporo,*

Hokkaido 060-8628, Japan; Institute for Chemical Reaction Design and Discovery (WPI-ICReDD), Hokkaido University, Sapporo, Hokkaido 001-0021, Japan; orcid.org/0000-0002-6622-8011; Email: hasegaway@eng.hokudai.ac.jp

Authors

Shota Hosoya – *Graduate School of Chemical Sciences and Engineering, Hokkaido University, Sapporo, Hokkaido 060-8628, Japan*

Takayuki Nakanishi – *Research Center for Electronic and Optical Materials, National Institute for Materials Science (NIMS), 1-1 Namiki, Tsukuba, Ibaraki 305-0044, Japan;* orcid.org/0000-0003-3412-2842

Masato Kobayashi – *Department of Chemistry, Faculty of Science, Hokkaido University, Sapporo, Hokkaido 060-0810, Japan; Institute for Chemical Reaction Design and Discovery (WPI-ICReDD), Hokkaido University, Sapporo, Hokkaido 001-0021, Japan;* orcid.org/0000-0002-4001-3581

Mengfei Wang – *Faculty of Engineering, Hokkaido University, Sapporo, Hokkaido 060-8628, Japan; Institute for Chemical Reaction Design and Discovery (WPI-ICReDD), Hokkaido University, Sapporo, Hokkaido 001-0021, Japan;* orcid.org/0000-0001-6171-8532

Koji Fushimi – *Faculty of Engineering, Hokkaido University, Sapporo, Hokkaido 060-8628, Japan*

Tetsuya Taketsugu – *Department of Chemistry, Faculty of Science, Hokkaido University, Sapporo, Hokkaido 060-0810, Japan; Institute for Chemical Reaction Design and Discovery (WPI-ICReDD), Hokkaido University, Sapporo, Hokkaido 001-0021, Japan;* orcid.org/0000-0002-1337-6694

Yuichi Kitagawa – *Faculty of Engineering, Hokkaido University, Sapporo, Hokkaido 060-8628, Japan; Institute for Chemical Reaction Design and Discovery (WPI-ICReDD), Hokkaido University, Sapporo, Hokkaido 001-0021, Japan;* orcid.org/0000-0003-1487-2531

Complete contact information is available at:
https://pubs.acs.org/10.1021/acs.inorgchem.

Author Contributions

The manuscript was written through contributions of all authors. All authors have given approval to the final version of the manuscript.

Notes

The authors declare no competing financial interest.

■ ACKNOWLEDGMENTS

This work was partially supported by JSPS KAKENHI Grant Numbers JP22K14741 (S.S.), JP23K17925 (Y.H.), JP22H02152 (Y.H.), JP22H04516 (Y.H.), JP20H02748 (Y.K.), and JP21K18969 (Y.K.). This work was also supported by 2021 and 2022 Feasibility Study Program of the Frontier Chemistry Center, Faculty of Engineering, Hokkaido University, and a Sumitomo Foundation Grant for Basic Science Research Project (S.S.). This work was also supported by the National Institute for Material Science (NIMS) Joint Research Hub Program and the Institute for Chemical Reaction Design and Discovery (ICReDD), established by the World Premier International Research Center Initiative (WPI) of MEXT, Japan. Some of the reported calculations were performed using computer facilities at the Research Center for Computational Science, Okazaki (Project: 23-IMS-C016).

■ REFERENCES

1. Wu, K.; Benchimol, E.; Baksi, A.; Clever, G. H. Non-Statistical Assembly of Multicomponent [Pd_2ABCD] Cages. *Nat. Chem.* **2024**,16, 584.
2. Takezawa, H.; Fujita, M. Molecular Confinement Effects by Self-Assembled

Coordination Cages. *Bull. Chem. Soc. Jpn.* **2021**, *94*, 2351–2369.

3. McTernan, C. T.; Davies, J. A.; Nitschke, J. R. Beyond Platonic: How to Build Metal–Organic Polyhedra Capable of Binding Low-Symmetry, Information-Rich Molecular Cargoes. *Chem. Rev.* **2022**, *122*, 10393–10437.
4. Wu, K.; Tessarolo, J.; Baksi, A.; Clever, G. H. Guest-Modulated Circularly Polarized Luminescence by Ligand-to-Ligand Chirality Transfer in Heteroleptic Pd^{II} Coordination Cages. *Angew. Chem. Int. Ed.* **2022**, *61*, e202205725.
5. Brzechwa-Chodzyńska, A.; Drożdż, W.; Harrowfield, J.; Stefankiewicz, A. R. Fluorescent Sensors: A Bright Future for Cages. *Coord. Chem. Rev.* **2021**, *434*, 213820.
6. Fang, Y.; Powell, J. A.; Li, E.; Wang, Q.; Perry, Z.; Kirchon, A.; Yang, X.; Xiao, Z.; Zhu, C.; Zhang, L.; Huang, F.; Zhou, H.-C. Catalytic Reactions within the Cavity of Coordination Cages. *Chem. Soc. Rev.* **2019**, *48*, 4707–4730.
7. Ham, R.; Nielsen, C. J.; Pullen, S.; Reek, J. N. H. Supramolecular Coordination Cages for Artificial Photosynthesis and Synthetic Photocatalysis. *Chem. Rev.* **2023**, *123*, 5225–5261.
8. Zhou, C.; Wang, X.; Xie, M.; Xia, R.; Luo, D.; Lian, Z.; Ning, G.; Lu, W.; Zhou, X.; Li, D. A Self-assembled Capsule for Propylene/Propane Separation. *Angew. Chem. Int. Ed.* **2023**, *62*, e202315020.
9. Zhang, D.; Ronson, T. K.; Zou, Y.-Q.; Nitschke, J. R. Metal–Organic Cages for Molecular Separations. *Nat. Rev. Chem.* **2021**, *5*, 168–182.
10. Xiao, Z.; Lin, H.; Drake, H. F.; Diaz, J.; Zhou, H. C.; Pellois, J. P. Investigating the Cell Entry Mechanism, Disassembly, and Toxicity of the Nanocage PCC-1: Insights into Its Potential as a Drug Delivery Vehicle. *J. Am. Chem. Soc.* **2023**, *145*, 27690–27701.
11. Casini, A.; Woods, B.; Wenzel, M. The Promise of Self-Assembled 3D Supramolecular Coordination Complexes for Biomedical Applications. *Inorg. Chem.*

2017, *56*, 14715–14729.

12. Jiao, Y.; Zuo, Y.; Yang, H.; Gao, X.; Duan, C. Photoresponse within Dye-Incorporated Metal-Organic Architectures. *Coord. Chem. Rev.* **2021**, *430*, 213648.
13. Zhao, J.; Zhou, Z.; Li, G.; Stang, J. P. Light-Emitting Self-Assembled Metallacages. *Natl. Sci. Rev.* **2021**, *8*, nwab045.
14. Shi, J.; Xu, W.; Yu, H.; Wang, X.; Jin, F.; Zhang, Q.; Zhang, H.; Peng, Q.; Abdurahman, A.; Wang, M. A Highly Luminescent Metallo-Supramolecular Radical Cage. *J. Am. Chem. Soc.* **2023**, *145*, 24081–24088.
15. Li, X.-Z.; Zhou, L.-P.; Hu, S.-J.; Cai, L.-X.; Guo, X.-Q.; Wang, Z.; Sun, Q.-F. Metal Ion Adaptive Self-Assembly of Photoactive Lanthanide-Based Supramolecular Hosts. *Chem. Commun.* **2020**, *56*, 4416–4419.
16. Yin, S.-Y.; Zhu, Y.-X.; Pan, M.; Wei, Z.-W.; Wang, H.-P.; Fan, Y.-N.; Su, C.-Y. Nanosized NIR-Luminescent Ln Metal–Organic Cage for Picric Acid Sensing. *Eur. J. Inorg. Chem.* **2017**, *2017*, 646–650.
17. Dou, W.-T.; Yang, C.-Y.; Hu, L.-R.; Song, B.; Jin, T.; Jia, P.-P.; Ji, X.; Zheng, F.; Yang, H.-B.; Xu, L. Metallacages and Covalent Cages for Biological Imaging and Therapeutics. *ACS Materials Lett.* **2023**, *5*, 1061–1082.
18. Li, X.-Z.; Tian, C.-B.; Sun, Q.-F. Coordination-Directed Self-Assembly of Functional Polynuclear Lanthanide Supramolecular Architectures. *Chem. Rev.* **2022**, *122*, 6374–6458.
19. Ning, Y.; Zhu, M.; Zhang, J.-L. Near-infrared (NIR) Lanthanide Molecular Probes for Bioimaging and Biosensing. *Coord. Chem. Rev.* **2019**, *399*, 213028.
20. Bünzli, J.-C. G. On the Design of Highly Luminescent Lanthanide Complexes. *Coord. Chem. Rev.* **2015**, *293–294*, 19–47.
21. Jin, G.-Q.; Sun, D.; Xia, X.; Jiang, Z.-F.; Cheng, B.; Ning, Y.; Wang, F.; Zhao, Y.; Chen, X.; Zhang, J.-L. Bioorthogonal Lanthanide Molecular Probes for Near-Infrared Fluorescence and Mass Spectrometry Imaging. *Angew. Chem. Int. Ed.*

2022, *61*, e202208707.

22. Ning, Y.; Liu, Y.-W.; Yang, Z.-S.; Yao, Y.; Kang, L.; Sessler, J. S.; Zhang, J.-L. Split and Use: Structural Isomers for Diagnosis and Therapy. *J. Am. Chem. Soc.* **2020**, *142*, 6761–6768.
23. Hu, J.-Y.; Ning, Y.; Meng, Y.-S.; Zhang, J.; Wu, Z.-Y.; Gao, S.; Zhang, J.-L. Highly Near-IR Emissive Ytterbium(III) Complexes with Unprecedented Quantum Yields. *Chem. Sci.* **2017**, *8*, 2702–2709.
24. Chan, W.-L.; Xie, C.; Lo, W.-S.; Bünzli, J.-C. G.; Wong, W.-K.; Wong, K-L. Lanthanide–Tetrapyrrole Complexes: Synthesis, Redox Chemistry, Photophysical Properties, and Photonic Applications. *Chem. Soc. Rev.* **2021**, *50*, 12189–12257.
25. Jin, G.-Q.; Chau, C. V.; Arambula, J. F.; Gao, S.; Sessler, J. L.; Zhang, J.-L. Lanthanide Porphyrinoids as Molecular Theranostics. *Chem. Soc. Rev*. **2022**, *51*, 6177–6209.
26. Zhang, Z.; Ma, L.; Fang, F.; Hou, Y.; Lu, C.; Mu, C.; Zhang, Y.; Liu, H.; Gao, K.; Wang, M.; Zhang, Z.; Li, X.; Zhang, M. Porphyrin-Based Multicomponent Metallacage: Host–Guest Complexation toward Photooxidation-Triggered Reversible Encapsulation and Release. *JACS Au* **2022**, *2*, 1479–1487.
27. Percástegui, E. G.; Jancik, V. Coordination-Driven Assemblies Based on *meso*-Substituted Porphyrins: Metal-Organic Cages and a New Type of *meso*-Metallaporphyrin Macrocycles. *Coord. Chem. Rev*. **2020**, *407*, 213165.
28. Durot, S.; Taesch, J.; Heitz, V. Multiporphyrinic Cages: Architectures and Functions. *Chem. Rev.* **2014**, *114*, 8542–8578.
29. Kishimoto, S.; Nakagawa, T.; Kawai, T.; Hasegawa, Y. Enhanced Near-Infrared Luminescence of Yb(III) Complexes with Phosphine Oxide and Hexafluoroacetylacetonate Ligands. *Bull. Chem. Soc. Jpn*. **2011**, *84*, 148–154.
30. Omagari, S.; Nakanishi, T.; Hirai, Y.; Kitagawa, Y.; Seki, T.; Fushimi, K.; Ito, H.; Hasegawa, Y. Origin of Concentration Quenching in Ytterbium Coordination

Polymers: Phonon-Assisted Energy Transfer. *Eur. J. Inorg. Chem.* **2018**, *2018*, 561–567.

31. Hasegawa, Y.; Kitagawa, Y. Thermo-Sensitive Luminescence of Lanthanide Complexes, Clusters, Coordination Polymers and Metal–Organic Frameworks with Organic Photosensitizers. *J. Mater. Chem. C* **2019**, *7*, 7494–7511.
32. Kitagawa, Y.; Suzue, F.; Nakanishi, T.; Fushimi, K.; Hasegawa, Y. A Highly Luminescent Eu(III) Complex Based on an Electronically Isolated Aromatic Ring System with Ultralong Lifetime. *Dalton Trans.* **2018**, *47*, 7327–7332.
33. Kitagawa, Y.; Nakai, T.; Hosoya, S.; Shoji, S.; Hasegawa, Y. Luminescent Lanthanide Complexes for Effective Oxygen-Sensing and Singlet Oxygen Generation. *ChemPlusChem* **2023**, *88*, e202200445.
34. Märkl, G.; Reiss, M.; Kreitmeier, P.; Nöth, H. *meso*-Tetrakis[4-(diphenylphosphino)-phenyl]porphyrin and a Water-Soluble Octakis-(phosphonium Salt) Porphyrin Double-Decker with a Cage Structure. *Angew. Chem. Int. Ed. Eng.* **1995**, *34*, 2230–2234.
35. Chen, H.; Roy, I.; Myong, M. S.; Seale, J. S. W.; Cai, K.; Jiao, Y.; Liu, W.; Song, B.; Zhang, L.; Zhao, X.; Feng, Y.; Liu, F.; Young, R. M.; Wasielewski, M. R.; Stoddart, J. F. Triplet–Triplet Annihilation Upconversion in a Porphyrinic Molecular Container. *J. Am. Chem. Soc.* **2023**, *145*, 10061–10070.
36. Spenst, P.; Würthner, F. A Perylene Bisimide Cyclophane as a “Turn-On” and “Turn-Off” Fluorescence Probe. *Angew. Chem. Int. Ed.* **2015**, *54*, 10165–10168.
37. Dale, E. J.; Vermeulen, N. A.; Thomas, A. A.; Barnes, J. C.; Juríček, M.; Blackburn, A. K.; Strutt, N. L.; Sarjeant, A. A.; Stern, C. L.; Denmark, S. E.; Stoddart, J. F. ExCage. *J. Am. Chem. Soc.* **2014**, *136*, 10669–10682.
38. Nakamura, T.; Ube, H.; Shionoya, M. Silver-Mediated Formation of a Cofacial Porphyrin Dimer with the Ability to Intercalate Aromatic Molecules. *Angew. Chem. Int. Ed.* **2013**, *52*, 12096–12100.

39. Bannwarth, C.; Caldeweyher, E.; Ehlert, S.; Hansen, A.; Pracht, P.; Seibert, J.; Spicher, S.; Grimme, S. Extended tight-binding quantum chemistry methods. *WIREs Comput. Mol. Sci.* **2021**, *11*, e1493.
40. Salazar, A.; Moreno-Simoni, M.; Kumar, S.; Labella, J.; Torres, T.; de la Torre, G. Supramolecular Subphthalocyanine Cage as Catalytic Container for the Functionalization of Fullerenes in Water. *Angew. Chem. Int. Ed*. **2023**, *62*, e202311255.
41. Contreras-García, J.; Johnson, E. R.; Keinan, S.; Chaudret, R.; Piquemal, J.-P.; Beratan, D. N.; Yang, W. NCIPLOT: A Program for Plotting Noncovalent Interaction Regions. *J. Chem. Theory Comput.* **2011**, *7*, 625–632.
42. Thordarson, P. Determining Association Constants from Titration Experiments in Supramolecular Chemistry. *Chem. Soc. Rev.* **2011**, *40*, 1305–1323.
43. Taniguchi, M.; Lindsey, J. S.; Bocian, D. F.; Holten, D. Comprehensive Review of Photophysical Parameters (ε, Φ_f, τ_s) of Tetraphenylporphyrin (H_2TPP) and Zinc Tetraphenylporphyrin (ZnTPP) – Critical Benchmark Molecules in Photochemistry and Photosynthesis. *J. Photochem. Photobiol, C: Photochem. Rev.*, **2021**, 46, 100401.
44. Inage, K.; Wang, M.; Hasegawa, Y.; Kitagawa, Y. Effective Photosensitized Emission of a Tb(III) Complex Using a β-diketonate Photosensitizer and an Oxygen Barrier System in a Thermally Populated Triplet State. *Dalton Trans*., **2024**, https://doi.org/10.1039/d4dt00286e.

For Table of Contents Only

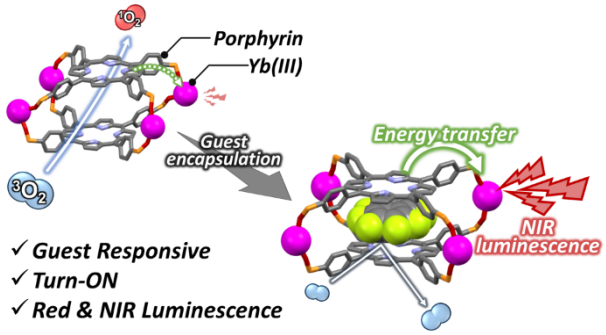

A novel NIR luminescent metal-organic-cage (MOC) composed of porphyrin dyes and Yb(III) complexes was synthesized. The host-guest packing between the MOC and the perfluoroaromatic guest molecules partially prevented oxygen molecules from approaching the cage and increased the NIR fluorescence intensity of the Yb(III) ion by the energy transfer from porphyrin to Yb(III) ion.